



MiR-101 Induces Senescence and Prevents Apoptosis in the Background of DNA Damage in MCF7 Cells

Siddharth Manvati¹, Kailash Chandra Mangalharra², P. Kalaiarasan¹, Niloo Srivastava², Bhupender Kumar², R. N. K. Bamezai^{2*}

¹ School of Biotechnology, Shri Mata Vaishno Devi University, Katra, Kakrayal, Jammu & Kashmir, India, ² National Centre of Applied Human Genetics, School of Life Sciences, Jawaharlal Nehru University, New Delhi, India

Abstract

Moderately increased DNA damage due to the exogenous miR-101 (4 fold) over-expression in MCF7 cells was substantiated by an increase in the number of γ -H2AX foci, correlating with a simple-to-do Halo-assay. miR-101 induced mild/moderate DNA damage favoured senescence rather than apoptosis. An experimental support emanated from the induced mild/moderate DNA damage with 1 μ M/5 μ M etoposide in MCF7 cells, which resulted in an endogenous miR-101 over-expression (10/4 fold, respectively), followed by senescence. On the other hand, the severe DNA damage induced with 10 μ M etoposide, resulted in a low (<1 fold) endogenous expression of miR-101 and an elevated percentage of apoptotic cells. Using bioinformatics tools along with *in-vitro* and *in-vivo* validations, miR-101 was found to target and downregulate the mRNA expression of UBE2N and SMARCA4, involved in DNA damage repair (DDR) pathways. Recovery of the expression of the two novel targets in anti-miR-101 transfection validated the results. We conclude that a threshold range of over-expressed miR-101, capable of inducing mild/moderate DNA damage, is sensed by cells to become senescent. The observation derives further support from *in-silico* protein-protein network analysis where the two novel targets showed their involvement in senescence pathway.

Citation: Manvati S, Mangalharra KC, Kalaiarasan P, Srivastava N, Kumar B, et al. (2014) MiR-101 Induces Senescence and Prevents Apoptosis in the Background of DNA Damage in MCF7 Cells. PLoS ONE 9(10): e111177. doi:10.1371/journal.pone.0111177

Editor: Alfons Navarro, University of Barcelona, Spain

Received: April 17, 2014; **Accepted:** September 25, 2014; **Published:** October 29, 2014

Copyright: © 2014 Manvati et al. This is an open-access article distributed under the terms of the Creative Commons Attribution License, which permits unrestricted use, distribution, and reproduction in any medium, provided the original author and source are credited.

Data Availability: The authors confirm that all data underlying the findings are fully available without restriction. All relevant data are within the paper and its Supporting Information files.

Funding: The study was funded by Jammu and Kashmir, Department of Science and Technology, Govt of India, through Shri Mata Vaishnov Devi University. The funders had no role in study design, data collection and analysis, decision to publish, or preparation of the manuscript.

Competing Interests: The authors have declared that no competing interests exist.

* Email: bamezai@hotmail.com

Introduction

MicroRNAs (miRNAs) are small non-coding RNA molecules (20–25 nucleotides long) that regulate gene expression at post-transcriptional level [1,2] by direct interaction at 5' or 3' UTR regions of target mRNA. The regulatory processes of miRNA, believed to involve around 60% of human genes [3], provide a new layer of regulation in gene expression. Understanding the role, therefore, of differential expression patterns of miRNA is of interest in cellular biology in general.

miR-101, one of the known microRNAs, was first reported to be down-regulated in prostate cancer and then in breast cancer cell lines, MCF7 and T47D, along with other miRNAs. The down-regulation of miR-101 was observed in several cancer types, such as Colorectal [4], Gastric, Lung [5], Bladder [6] and Breast Cancer [7]. Despite the knowledge about several of its targets, the direct mechanistic role of miR-101 in cancer and its specific interaction after the change in expression within a given pathway has remained elusive. Reports have also suggested an increase in expression of miR-101 under radiation induced DNA damage conditions [8]; and hypothesized its probable role in cellular senescence [9], not proven unequivocally. Here, we ascertain the role of this microRNA in inducing DNA damage which when mild/moderate guides the cells towards senescence

instead of apoptosis. This biological role of miR-101 apparently is novel and of interest.

Results

miR-101 over-expression induces DNA Damage

A four-fold increase in miR-101 expression in transiently transfected MCF7 cells resulted in DNA damage, as assessed by the presence of an increased number of γ H2AX foci and correlated with a simple-to-do Halo assay (Figure 1a), allowing semi-quantification through an increased nuclear diffusion factor (NDF) analysis. NDF values in miR-101 over-expressing cells showed a considerable increase (6.2 ± 1.5) as compared to mock transfected (1.6 ± 1.5) and etoposide (1 μ M) treated cells, used as a positive control (4.4 ± 1.5) (Figure 1b). The average number of γ H2AX foci increased in miR-101 over-expressing cells (16 ± 3) as compared to mock transfected (4 ± 1) and the positive control (11 ± 4) cells (Figure 1c), indicating the involvement of miR-101 in inducing DNA damage. The etoposide (1 μ M) induced DNA damage in MCF-7 cells also resulted in an increased (10-Fold) endogenous expression of miR-101 (Figure 1d). The 4 to 10 fold exogenous or etoposide induced endogenous expression of miR-101, respectively, suggested the involvement of a threshold range of miR-101 in inducing mild/moderate DNA damage in the cell.

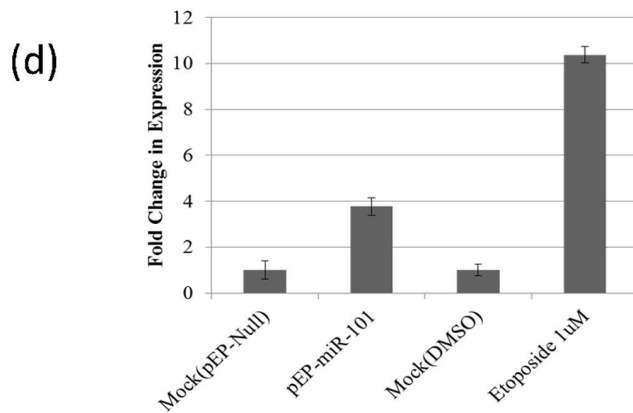
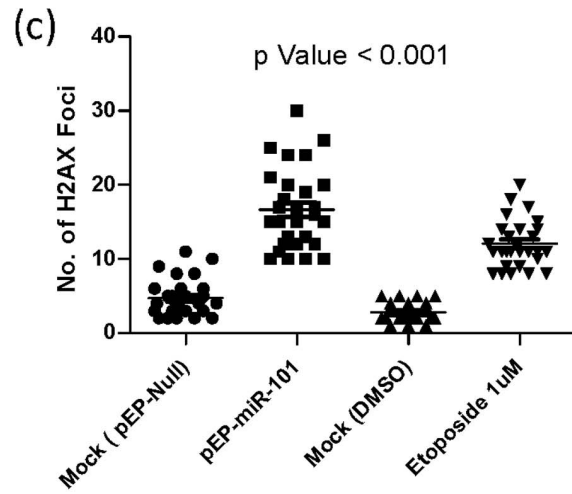
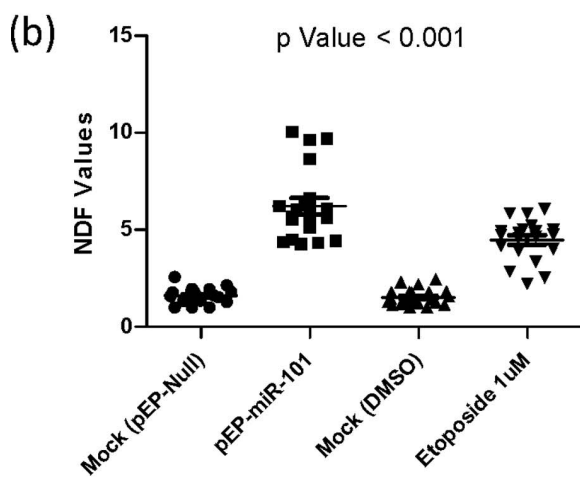
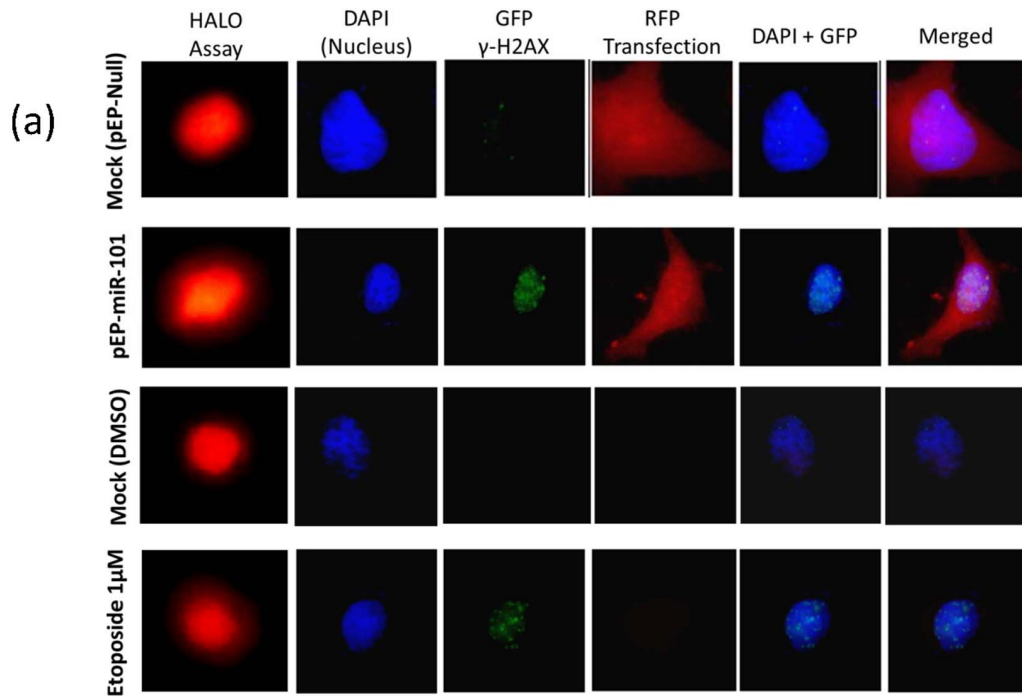


Figure 1. Visualization, quantification of DNA damage, and fold change in expression of miR-101 in MCF7 cells. (a) Fluorescence microscopy where six columns represent - Halo Assay used for calculating NDF values, DAPI staining for nucleus, γ H2AX foci with GFP tagged secondary antibodies, RFP-tagged pEP-Vector, Merged-DAPI+GFP-tagged γ H2AX and Merged-DAPI+ GFP-tagged γ H2AX+ RFP-tagged pEP-Vector; (b) NDF values representing the extent of diffusion of damaged DNA in cells (Halo assay) [27]; (c) number of γ H2AX foci; (d) fold change in expression of miR-101, in Controls: mock-pEP-Null-transfected, mock-DMSO treated, and Experimental conditions: pEP-miR-101 transfection and Etoposide 1 μ M treatment.

doi:10.1371/journal.pone.0111177.g001

miR-101 promotes senescence but not apoptosis

Exogenously over-expression of miR-101 and etoposide (1 μ M) induced endogenous expression of miR-101 in cells, resulting in mild/moderate DNA damage, was compared for the rate of cellular senescence or apoptosis. An absence of a significant difference in apoptotic cell population was noted between over-expressing miR-101 (15 \pm 2%), mock transfected control (17 \pm 2%), and etoposide treated (20 \pm 2%) cells. Whereas, inhibition of miR-101, using anti-miR oligonucleotides, increased the percentage of apoptotic cells significantly (30 \pm 2%) ($p < 0.05$) (Figure 2 a & b).

The number of senescent cells under similar conditions, however, showed a significant increase in miR-101 over-expressing (1.8-Fold \pm 0.25) also observed in 1 μ M etoposide exposed (1.5-Fold \pm 0.25) MCF7 cells, when compared to mock transfected controls ($p < 0.05$). Further, continuous (upto 72 hrs) over-expression of miR-101 depicted an enhanced induction of senescence (2.3-Fold \pm 0.25). miR-101 inhibition with anti-miR-101 oligonucleotides depicted a profile (0.9-Fold \pm 0.25) (Figure 2 c & d) which matched with the control cells. Further validation was carried out in experiments with well-established concentrations (1 μ M, 5 μ M and 10 μ M) of etoposide inducing differential levels of DNA damage in MCF7 cells, which were assayed for (i) senescence, (ii) apoptosis and (iii) miR-101 expression. With an increasing DNA damage (average NDF values: 1 μ M : 4, 5 μ M : 5 and 10 μ M : 8 in Halo assay) (Figure 3a), a concomitant decrease in the percentage of senescent cells (1 μ M : 65 \pm 2%, 5 μ M : 63 \pm 2% and 10 μ M : 46 \pm 2%; $p < 0.05$) and an increase in Annexin-V positive apoptotic cells (1 μ M : 35 \pm 2%, 5 μ M : 37 \pm 2% and 10 μ M : 54 \pm 2%; $p < 0.05$) (Figure 3b) was observed. Inhibition of miR-101 (with anti-miR-101) in 1 μ M etoposide treated cells resulted in an increase in the percentage of annexin-V positive cells and a decrease in senescent cells (Figure S1 in File S1), supporting our observations.

The decrease in the endogenous expression of miR-101 experimentally with increasing doses of etoposide (1 μ M: 10-Fold, 5 μ M : 2-Fold and 10 μ M : 0.5-Fold; $p < 0.005$) (Figure 3c) correlated negatively with the induced DNA damage (Figure 3a) and the rate of apoptosis (Figure 3c). And, the results were positively correlated with increasing senescence (Figure 3c). Since, the generation of stable lines with miR-101 did not succeed; we assumed that a constitutive expression was not in favour of cell survival.

miR-101 targets 3'UTR of UBE2N and SMARCA4

In order to unravel the probable mechanism involved in miR-101 mediated DNA damage, gene specific targets of miR-101 were identified bio-informatically (Figure 4a) by three target prediction programs (described under Materials and Methods section). These targets were validated by *in-vitro* Dual-Luciferase Reporter Assays and the activity of luciferase measured from Luc gene in presence of 3'UTR binding site of UBE2N and SMARCA4, independently for the two genes, in presence of miR-101. The significantly decreased reporter gene activity in MCF7 cells ($p = 0.001$ & 0.005) and replicated in HeLa cells ($p = 0.00019$ & 0.000142), when compared to the control experiments where 3'UTR-binding-site was absent (Figure 4b), confirmed UBE2N and SMARCA4 as targets of miR-101. The validation of the two targets, UBE2N and

SMARCA4, was established by measuring their endogenous cellular expression as well, which decreased significantly in over-expressing miR-101 cells (Figure 4c). The role of miR-101 in targeting these was further supported when etoposide (10 μ M)-induced decrease in endogenous expression of miR-101 resulted in increased endogenous expression of the two cellular targets, UBE2N (1 μ M : 0.003-Fold, 5 μ M : 5-Fold and 10 μ M : 16-Fold) and SMARCA4 (1 μ M : 0.04-Fold, 5 μ M : 6-Fold and 10 μ M : 21-Fold) (Figure 4d). This concentration (10 μ M) of etoposide not only induced low levels of miR-101 but also increased the rate of apoptosis, suggesting the least involvement of the miRNA in apoptotic processes.

In-silico protein-protein network analysis identified that the experimentally validated novel targets of miR-101, SMARCA4 and UBE2N, interact with proteins of DDR and senescence pathways via TP53 and RB1. One of the DDR pathway protein H2AFX, known to form complex with RNF8 [10,11], was reported to be ubiquitinated by UBE2N [12] (Figure 5). *In-silico* network analysis also reflected a link between DDR and apoptosis related genes, as observed in experiments where, etoposide (10 μ M) induced severe DNA damage resulted in low miR-101 expression and a high apoptotic rate. This process, *in-silico* and in experiments, did not involve the studied two targets of miR-101, suggesting the apoptotic induction to followed an independent path sever DNA damage in the cells.

Discussion

A sequential role of miR-101 in inducing mild/moderate DNA damage followed by senescence in MCF7 cells was observed which has not been proposed earlier. Two independent experimental conditions, one of exogenous over-expression and second of endogenous induction with 1 μ M etoposide of miR-101 in the cells, resulted in mild/moderate DNA damage and senescent cells. We propose that miR-101 is one amongst many of the candidates within the cellular milieu, which plays a significant role in initiating senescence and not apoptosis. The observations made by us lend support to the hypothesized role of miR-101 induced senescence [9,13,14] through DNA damage [15]. This event of senescence in a cell apparently happens under the condition of a mild/moderate DNA damage induced in a cell, which is shifted to apoptotic path in case the damage induced is severe.

The reversal of the phenomenon under anti-miR-101 experimental conditions, in presence of high dose (10 μ M) of etoposide, where senescence decreased and apoptosis increased supported the role of miR-101 in senescence and not in apoptosis, the latter following an independent path. A decrease in the cellular mRNA expression of the two novel targets involved in DDR pathway, SMARCA4 and UBE2N, coincided with a 4–10 fold exogenous or endogenous expression of miR-101, resulting in mild/moderate DNA damage in cells which acquired senescence. Further increase in senescence in *in-vitro* experiments with longer exposure time of 72 hrs to exogenous over-expression of miR-101, supported the conclusions drawn. *In-silico* protein-protein network analysis, to look for the role of SMARCA4 and UBE2N and its interacting partners in DDR, senescence and apoptosis pathways revealed that P53 and Rb proteins interact with SMARCA4, the target

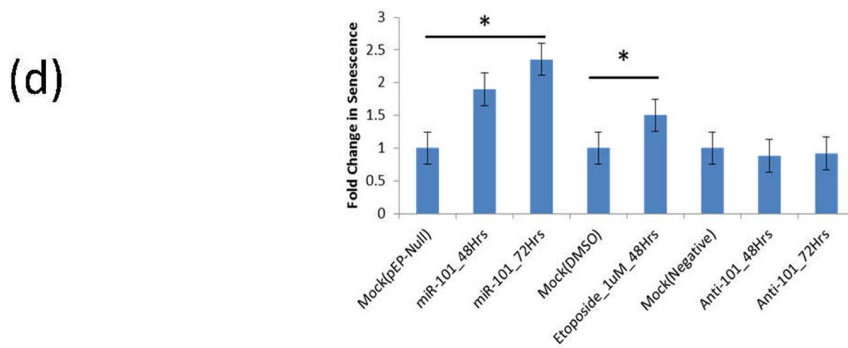
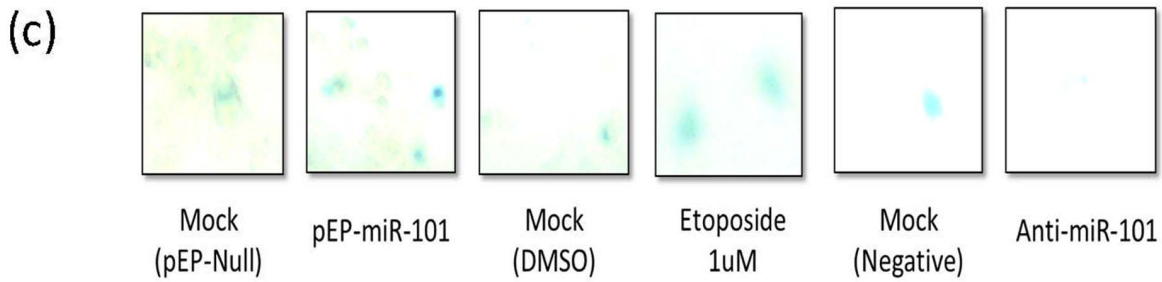
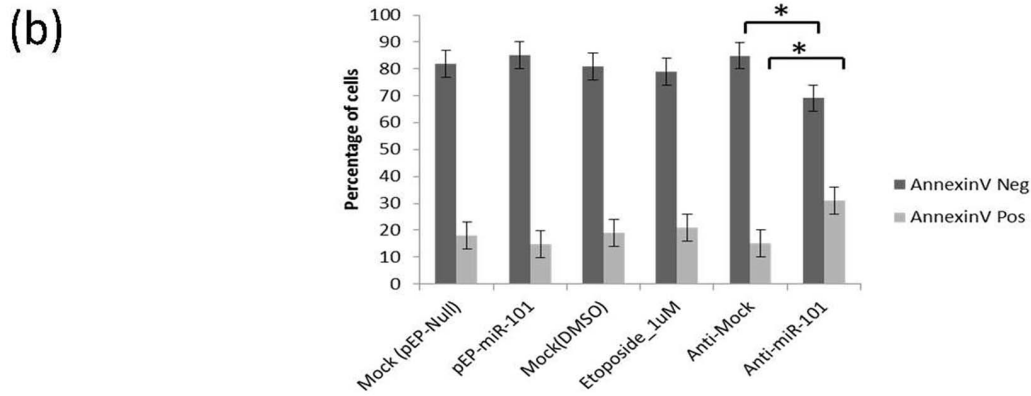
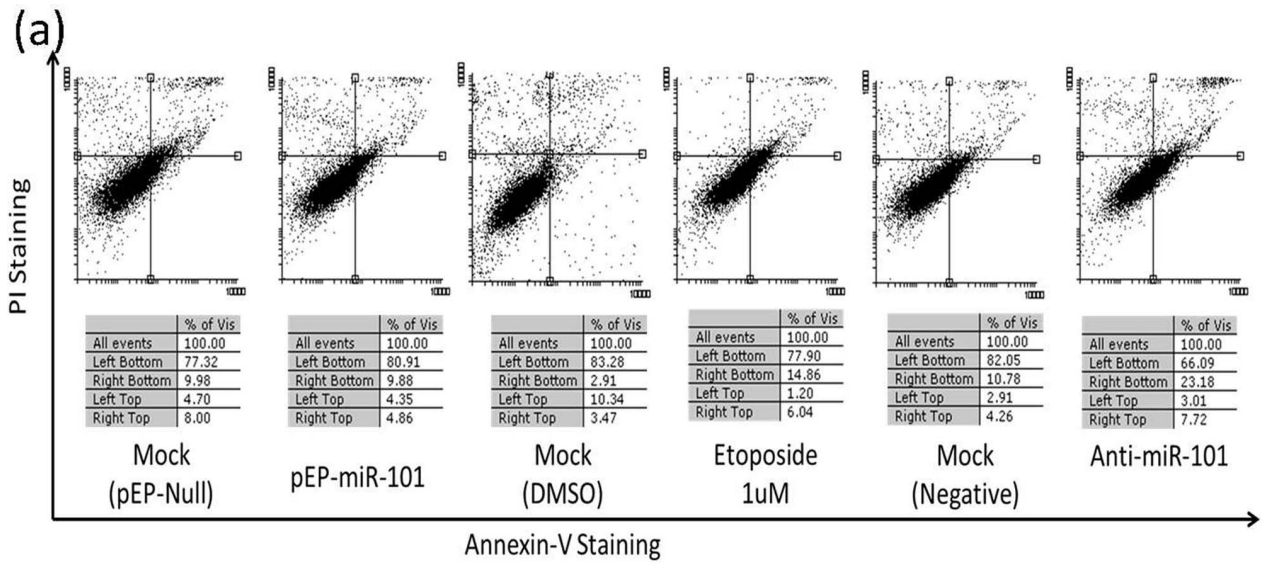


Figure 2. miR-101 induces senescence and not apoptosis in MCF7 cells. (a) Original Flow-cytometry dot-blot of PI Staining Vs Annexin-V Staining, (b) Percentage of Annexin-V positive (apoptotic) and negative cells, (c) β -gal positively stained (senescent) cells, (d) Fold change in number of senescent cells, under control (mock-pEP-Null-transfected, mock-DMSO treated & mock negative with scrambled primers) and experimental conditions (pEP-miR-101 transfection, Etoposide 1 μ M treatment & anti-miR-101 transfection). Time dependent increase in senescence in miR-101 transfected cells is also shown (d).
doi:10.1371/journal.pone.0111177.g002

gene of miR-101. P53 and Rb have been implicated in senescence [16–18] besides their role in cell death [19,20] and survival [18,21]. SMARCA4 (BRG1) has been implicated in cellular

senescence by regulating pRb activity directly or through upregulation of p21 [22]. Same is true for UBE2N, where MDC1 and H2AX complex, ubiquitinated by UBE2N [23] would fail to

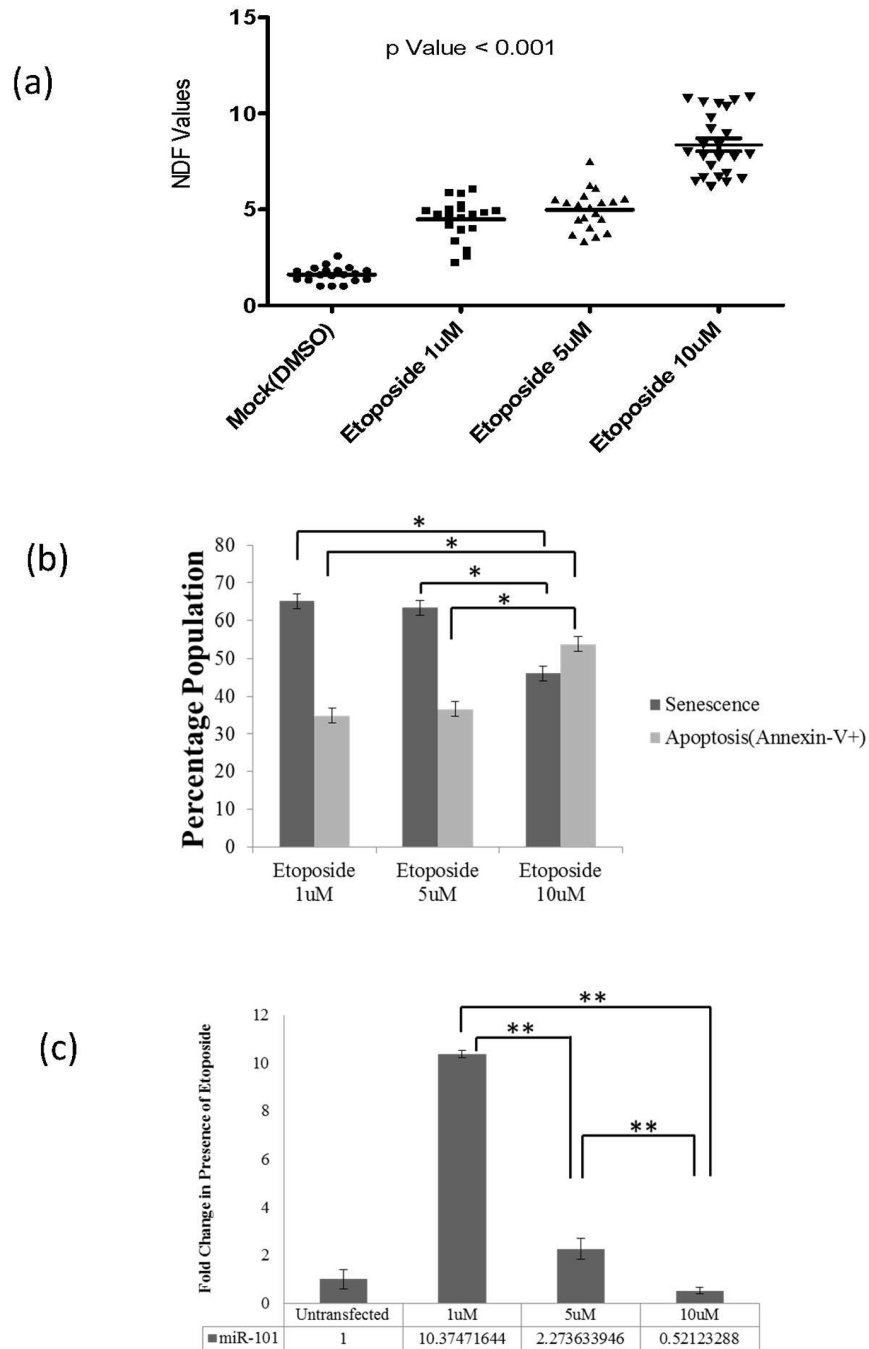


Figure 3. Halo assay performed in MCF7 cells. (a) NDF-nuclear diffusion factor-values showing the extent of DNA damage with increasing concentrations of etoposide (p Value <0.001), (b) Percentage of senescent cell population (using β -gal assay) and Annexin-V positive-apoptotic-cell population (through FACS analysis): showing decrease in senescence and increase in Apoptosis (*p Value <0.05), (c) miR-101 expression (using Real-Time PCR): showing decrease with increasing concentration of etoposide (1 μ M, 5 μ M and 10 μ M) for 12 hrs (**p Value <0.005).
doi:10.1371/journal.pone.0111177.g003

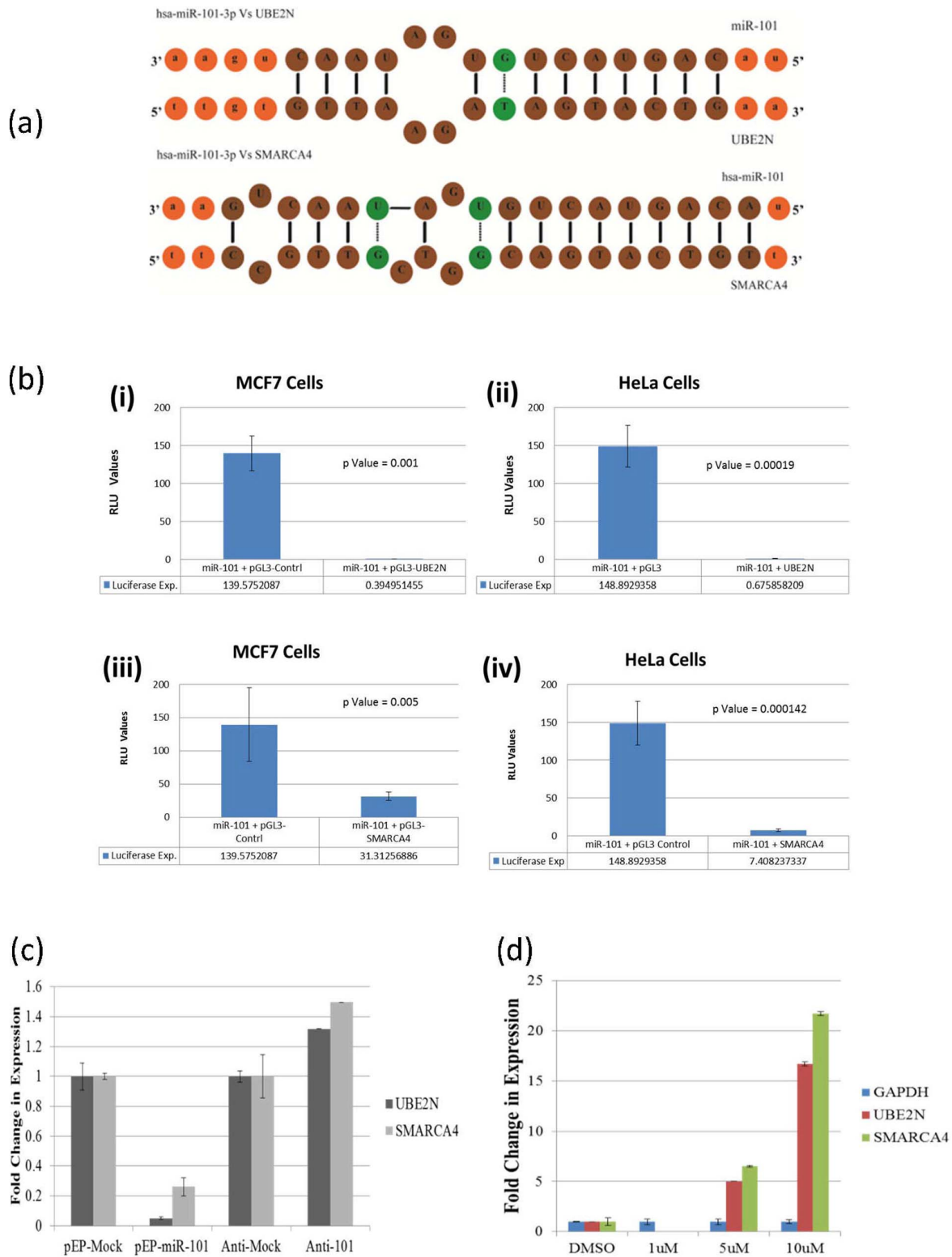


Figure 4. UBE2N and SMARCA4 as novel targets of miR-101. (a) Bio-informatics revealing the presence of miR-101 binding site at 3'UTR of UBE2N and SMARCA4, (b) activity of Luc gene showing a significant decrease in Luciferase activity when miR-101 was over-expressed in cells expressing Luc with 3'UTR of either (i & ii) UBE2N or (iii & iv) SMARCA4, in MCF7 and HeLa cells. (c & d) Real-Time PCR showing a change in expression using Sybergreen and UBE2N and SMARCA4 specific primers, (c) under miR-101 and anti-miR-101 transfected conditions, showing decrease & increase, respectively, and (d) after 12 hrs exposure to 1uM, 5 uM and 10 uM etoposide, in MCF7 cells, confirming UBE2N and SMARCA4 as targets of miR-101, which is induced to 10 fold with 1 uM etoposide. At the higher concentrations of etoposide miR-101 expression is reduced leading to increased expression of UBE2N and SMARCA4, again confirming the relationship between miR-101 and the two novel targets. doi:10.1371/journal.pone.0111177.g004

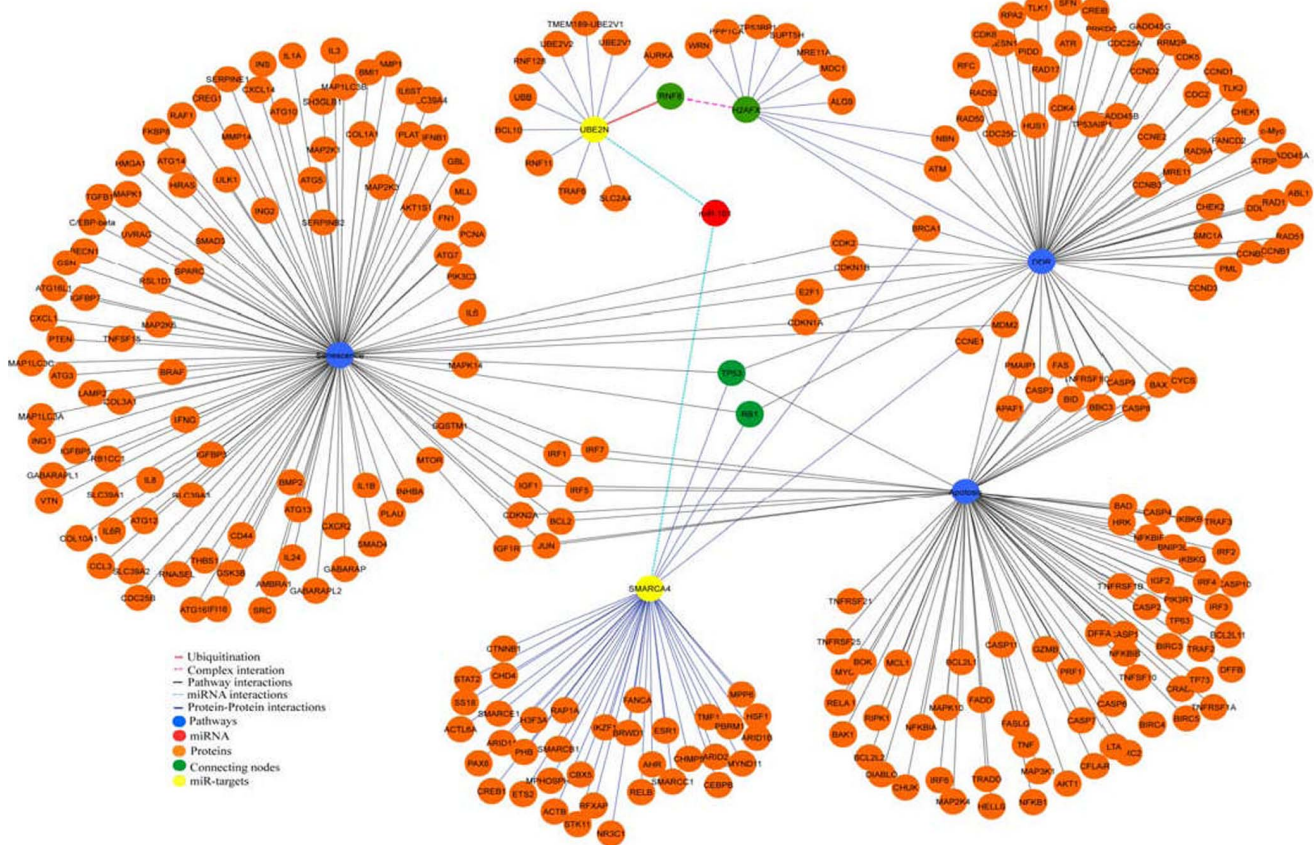


Figure 5. Protein-Protein network interaction of SMARCA4 and UBE2N as targets of miR-101 and as partners of proteins involved in DDR & senescence. Network explains the interaction of SMARCA4 and UBE2N with DDR pathway. SMARCA4 is shown to be involved in DDR and senescence pathways through RB1 and TP53. RNF8 forms a complex with H2AFX which is highlighted in pink colour edge and the ubiquitination of RNF8 by UBE2N is shown in red colour edge. All the nodes and edges of protein-protein interaction are in orange and violet colour respectively. The connecting key molecules in the network are highlighted as green. Pathway interaction nodes and edges are in blue and black colour respectively. The coloured node miR-101 which was predicted to target yellow-coloured-nodes, SMARCA4 and UBE2N, are highlighted by cyan colour edges. doi:10.1371/journal.pone.0111177.g005

activate cell survival pathway, unable to form a complex with SMARCA4, RAP80, BRCA1, CCNDC98, to activate transcription of protein molecules involved in chromatin remodeling [19].

It would be interesting to understand in future if such senescent cells with mil/moderate DNA damage, could turn tumorigenic, since senescent cells have been reported to attain this characteristic [24]. Our study suggests, though the decisions towards neoplastic transformation or apoptosis may not necessarily be regulated by miR-101 alone; nevertheless its role in senescence after inducing a moderate DNA damage remains interesting.

Materials and Methods

miR-101 cloning in expression vector

miR-101 expressing vectors were generated using pre-miR amplicon of miR-101 from genomic DNA and pEP-miR vector (Cell Biolabs) as backbone. The pre-miR sequence was obtained using primer sets (Table S2 in File S1) and amplified from human genomic DNA by simple PCR reaction. The primers (IDT) were designed using online (Primer 3) and offline (Oligo) tools such that the 5' ends of each forward and reverse primer contained Nhe-I and BamH1 restriction sites, respectively. These sites were also identified in pEP-miR vector for cloning purposes. After

amplification the product was digested and cloned into pEP-miR vector, generating pEP-miR-101 recombinant clone.

DNA damage induction and assays

Both miR-101 for exogenous (after transfection) and etoposide, one of the widely studied agents [25,26], for endogenous induction of DNA Damage (as assessed in the present work), were used for experimentation. Cells were seeded and harvested in 6-well plate and supplemented with DMEM Medium with 10% FBS. After 24 hrs of seeding, the media was replaced with fresh DMEM with 10% FBS containing 1 μM/5 μM/10 μM concentrations of Etoposide, for 12 hrs. Etoposide powder was dissolved in DMSO according to manufacturer's protocol.

Fast Halo Assay. After exogenous (miR-101) and endogenous (etoposide) induction of DNA damage, cells were suspended in ice-cold PBS containing 5 mmol/L EDTA and the suspension diluted with an equal volume of 2% low-melting agarose in PBS and immediately sandwiched between an agarose-coated slide and a coverslip. After complete gelling on ice, the coverslips were removed and the slides were immersed in 0.3 mol/L NaOH for 15 min at room temperature. Ethidium bromide (10 μg/mL) was directly added during the last 5 min of incubation [27]. The slides were then washed and de-stained for 5 min in distilled water. The ethidium bromide-labeled DNA images were acquired using a

Fluorescence microscopy (IX81, Olympus) and processed with image analysis software (Image J). The extent of damage was quantified by calculating the nuclear diffusion factor (NDF), which represents the ratio between the total area of the halo plus nucleus and that of the nucleus.

γ H2AX-Foci assay. In order to validate the extent of exogenously and endogenously induced DNA damage and correlate with the Halo-assay, the cells were fixed in 3% paraformaldehyde (PFA) (Sigma) in PBS (Sigma) for 15 min. Thereafter, cells were put in PBS (Sigma) and permeabilised on ice with 0.2% Triton X-100 (Qualigen) in PBS (Sigma). Cells were washed three times in PBS (Sigma) containing 1% of Chicken Bovine Serum Albumine (BSA). Subsequently the staining was performed with a primary rabbit raised anti- γ -H2AX antibody (phosphorylated at Ser 139) (1:300) (Invitrogen) for 1 h. After washing the cells three times in PBS (Sigma) containing 1% of Chicken BSA, the slides were incubated with a GFP tagged-polyclonal chicken anti-rabbit antibody (1:1000) (Invitrogen) overnight. Afterwards, the slides were rinsed four times in PBS (Sigma). Finally, to counterstain the nucleus, 35 ml slow-fade mounting medium containing 2% 40,6-Diamidino-2-Phenylindole (DAPI) (Sigma) was dropped on the cells and slides were covered with a coverslip. Slides were scored for γ H2AX-foci and preserved in a cool and dark place to allow the mounting medium to dry and to avoid fast fading of the fluorescent signal [28].

Images were viewed using Cell^{AF} Software and captured using digital camera of Olympus fluorescent microscope. All images were identically processed using auto features of the Cell^{AF} Software which has been used in automation of image analysis for Fluorescence microscopy. Only foci within the DAPI stained nucleus were counted. Deformed or fragmented nuclei, presumably corresponding to apoptotic cells, were excluded from the analysis. The vector used for transfection was RFP tagged and helped identify transfected cells. Cells were visualized by Olympus fluorescence microscope (IX81, Olympus). A minimum of two images (~15 to 50 cells per image) were taken randomly of each of four slides at 100X magnification.

Apoptotic Assay

Apoptosis was measured by the flow-cytometer detection of phosphatidylserine externalization using APC Annexin V staining (BD Biosciences, MD). MCF-7 cells, after transfection with pre-miR-101, anti-miR-101 and control miRs, were harvested and processed for APC Annexin V staining as per the manufacturer's protocol (BD Biosciences). Briefly, cells were washed twice with binding buffer (10 mmol/l (4-(2-hydroxyethyl)-1-piperazineethanesulfonic acid, 140 mmol/l NaCl and 5 mmol/l CaCl₂, pH 7.4) and stained with APC-conjugated annexin V for 15 minutes at room temperature, followed by flow-cytometer analysis using the Becton Dickinson FACS Calibur (Franklin Lakes). The extent of apoptosis was quantified as the percentage of annexin V-positive cells [29].

Senescence Assay

β -galactosidase assay allows the identification of senescent cells in mammalian culture cells [30]. Sub-confluent cells were washed twice with enough PBS to comfortably cover the cells (~2 ml per 35 mm dish) for ~30 s per wash. Enough fixation solution was added to submerge the cells (1–2 ml per 35 mm dish); and incubated for 5 min at room temperature. The fixation solution contained proportions of formaldehyde and glutaraldehyde, which are toxic and corrosive. The fixation solution was removed and fixed cells were washed twice with PBS. Staining solution (1–2 ml per 35 mm dish) was added and incubated overnight (12–16 h) at

37°C. After the incubation, the cells were washed for ~30 s twice with PBS (2 ml per 35 mm dish), and once with methanol (1 ml per 35 mm dish) and air dried. The stained cells were viewed by bright field or phase contrast microscopy.

Target Prediction & Validation

Bioinformatics prediction. The targets for miR-101 were predicted using three target prediction program (miRanda 3.3a [31], TargetScan 6.2 [32] and RNAhybrid 2.1 [33]). Fasta sequence of hsa-miR-101 was retrieved from miRBase. The binding site in the predicted targets for miR-101 was scanned using default parameters in all three software's. 3'UTR sequences of SMARCA4 and UBE2N genes were retrieved from UCSC genome table browser. To identify the relationship between the DDR pathway with SMARCA4 and UBE2N, we constructed the network using cytoscape [34]. The DDR and senescence pathway proteins were retrieved from wiki pathway [35] and HPRD [36] database used to retrieve interacting protein of SMARCA4 and UBE2N.

Reporter Assay & target validation. The 3'UTR of novel targets, established bio-informatically, were cloned into the 3'UTR of pGL3-Control vector (Promega) at Xba-I site. The 3'UTR was amplified from human genomic DNA, using primer (IDT) sets (Table S1 in File S1). The amplicons were then cloned, generating pGL3-UBE2N & pGL3-SMARCA4 vectors. All the clones were verified for containing the desired insert, by colony PCR, restriction digestion and DNA sequencing. Both pGL3 control and pEP-miR-101 (The miR-101 expressing vector) constructs were co-transfected in two different cell lines, MCF7 and HeLa. The transfection was performed using ESCORT'S (Sigma-Aldrich) reagent and according to manufacturer's protocol. The assay was performed after seeding in MCF7 and HeLa cells, in a 24-well plate, using Dual-Luciferase Assay Kit (Promega). After 48 hrs of transfection the cells were measured for Firefly and Renilla luminescence, using luminometer. The ratio of Firefly and Renilla reporter in presence of pEP-miR-101 was calculated and used in defining the change in expression of Firefly reporter in co-presence of predicted binding sites of specific genes.

RNA isolation and quantitative-PCR for miR-101 & target gene expression. RNA was isolated using TRIzol (Sigma) method and the quality and quantity verified by formaldehyde gel electrophoresis and Nanodrop (ND-1000, Nanodrop), respectively. cDNA preparation was carried out, using the High-Throughput cDNA Preparation kit (Part No-4368813, Life Technologies), following manufacturer's protocol, using 5 ng of RNA for cDNA synthesis of microRNA. TaqManRNU44 and has-miR-101 assays were performed by real time PCR. SYBR green Real-Time PCR was performed using SYBR Green reaction mix and UBE2N & SMARCA4 specific primers, designed using both online and offline tools, i.e. primer 3 and Oligo, respectively. Target (miR-101) and reference (RNU44) genes were amplified using ABI PRISM 7000 sequence detection system (Applied Biosystems). For all Real-Time PCR reactions the threshold cycle (Ct) was obtained using SDS 1.1 RQ software (Applied Biosystems). The fold change in expression of the target microRNAs and the reference genes was calculated using Delta Delta Ct ($\Delta\Delta$ Ct) method. RNU44 was selected as the endogenous control for microRNA expression analysis, whereas for gene expression analysis GAPDH was selected as the endogenous control.

Statistical Analysis

The results obtained through Becton Dickinson FACS Calibur were analysed using Flowing software. The p values for miR

expression were calculated, using Kruskal-Wallis test; and for luciferase assay by One-Way ANOVA.

Supporting Information

File S1 Figure S1, (a) Percentage of annexin-v positive cells and (b) fold change in senescence in MCF7 cells, treated with 1 μ M etoposide independently and in combination with anti-miR-101. **Table S1**, Score of targets predicted by prediction tools. **Table S2**, List of primers used for cloning purpose. (DOCX)

References

- Hibio N, Hino K, Shimizu E, Nagata Y, Ui-Tei K (2012) Stability of miRNA 5' terminal and seed regions is correlated with experimentally observed miRNA-mediated silencing efficacy. *Sci Rep* 2: 996.
- Gregory RI, Chendrimada TP, Shickhattar R (2006) MicroRNA biogenesis: isolation and characterization of the microprocessor complex. *Methods Mol Biol* 342: 33–47.
- Farh KK, Grimson A, Jan C, Lewis BP, Johnston WK, et al. (2005) The widespread impact of mammalian MicroRNAs on mRNA repression and translation. *Science* 310: 1817–1821.
- Strillacci A, Griffoni C, Sansone P, Paterini P, Piazza G, et al. (2009) MiR-101 downregulation is involved in cyclooxygenase-2 overexpression in human colon cancer cells. *Exp Cell Res* 315: 1439–1447.
- Sandberg AA, Meloni-Ehrig AM (2010) Cytogenetics and genetics of human cancer: methods and accomplishments. *Cancer Genet Cytogenet* 203: 102–126.
- Friedman JM, Liang G, Liu CC, Wolff EM, Tsai YC, et al. (2009) The putative tumor suppressor microRNA-101 modulates the cancer epigenome by repressing the polycomb group protein EZH2. *Cancer Res* 69: 2623–2629.
- Zhao L, Sun Y, Hou Y, Peng Q, Wang L, et al. (2012) MiRNA expression analysis of cancer-associated fibroblasts and normal fibroblasts in breast cancer. *Int J Biochem Cell Biol* 44: 2051–2059.
- Chen S, Wang H, Ng WL, Curran WJ, Wang Y (2011) Radiosensitizing effects of ectopic miR-101 on non-small-cell lung cancer cells depend on the endogenous miR-101 level. *Int J Radiat Oncol Biol Phys* 81: 1524–1529.
- Xiaoping L, Zhibin Y, Wenjuan L, Zeyou W, Gang X, et al. (2013) CPEB1, a histone-modified hypomethylated gene, is regulated by miR-101 and involved in cell senescence in glioma. *Cell Death Dis* 4: e675.
- Mattiroli F, Vissers JH, van Dijk WJ, Ikpa P, Citterio E, et al. (2012) RNF168 ubiquitinates K13-15 on H2A/H2AX to drive DNA damage signaling. *Cell* 150: 1182–1195.
- Mok MT, Henderson BR (2012) Three-dimensional imaging reveals the spatial separation of gammaH2AX-MDC1-53BP1 and RNF8-RNF168-BRCA1-A complexes at ionizing radiation-induced foci. *Radiother Oncol* 103: 415–420.
- Plans V, Scheper J, Soler M, Loukili N, Okano Y, et al. (2006) The RING finger protein RNF8 recruits UBC13 for lysine 63-based self polyubiquitylation. *J Cell Biochem* 97: 572–582.
- Greussing R, Hackl M, Charoentong P, Pauck A, Monteforte R, et al. (2013) Identification of microRNA-mRNA functional interactions in UVB-induced senescence of human diploid fibroblasts. *BMC Genomics* 14: 224.
- Tzatsos A, Paskaleva P, Lympieri S, Contino G, Stoykova S, et al. (2011) Lysine-specific demethylase 2B (KDM2B)-let-7-enhancer of zester homolog 2 (EZH2) pathway regulates cell cycle progression and senescence in primary cells. *J Biol Chem* 286: 33061–33069.
- d'Adda di Fagagna F (2008) Living on a break: cellular senescence as a DNA-damage response. *Nat Rev Cancer* 8: 512–522.
- Psyrrri A, DeFilippis RA, Edwards AP, Yates KE, Manuclidis L, et al. (2004) Role of the retinoblastoma pathway in senescence triggered by repression of the human papillomavirus E7 protein in cervical carcinoma cells. *Cancer Res* 64: 3079–3086.
- Rufini A, Tucci P, Celardo I, Melino G (2013) Senescence and aging: the critical roles of p53. *Oncogene* 32: 5129–5143.
- Das S, Boswell SA, Aaronson SA, Lee SW (2008) P53 promoter selection: choosing between life and death. *Cell Cycle* 7: 154–157.
- Bochar DA, Wang L, Beniya H, Kinev A, Xue Y, et al. (2000) BRCA1 is associated with a human SWI/SNF-related complex: linking chromatin remodeling to breast cancer. *Cell* 102: 257–265.
- Collard TJ, Urban BC, Patsos HA, Hague A, Townsend PA, et al. (2012) The retinoblastoma protein (Rb) as an anti-apoptotic factor: expression of Rb is required for the anti-apoptotic function of BAG-1 protein in colorectal tumour cells. *Cell Death Dis* 3: e408.
- Alessio N, Bohn W, Rauchberger V, Rizzolio F, Cipollaro M, et al. (2013) Silencing of RB1 but not of RB2/P130 induces cellular senescence and impairs the differentiation potential of human mesenchymal stem cells. *Cell Mol Life Sci* 70: 1637–1651.
- Kang H, Cui K, Zhao K (2004) BRG1 controls the activity of the retinoblastoma protein via regulation of p21CIP1/WAF1/SDI. *Mol Cell Biol* 24: 1188–1199.
- Bonner WM, Redon CE, Dickey JS, Nakamura AJ, Sedelnikova OA, et al. (2008) GammaH2AX and cancer. *Nat Rev Cancer* 8: 957–967.
- Campisi J (2013) Aging, cellular senescence, and cancer. *Annu Rev Physiol* 75: 685–705.
- Hogstrand K, Bohme J (1999) DNA damage caused by etoposide and gamma-irradiation induces gene conversion of the MHC in a mouse non-germline testis cell line. *Mutat Res* 423: 155–169.
- Li Z, Sun B, Clewell RA, Adeleye Y, Andersen ME, et al. (2013) Dose Response Modeling of Etoposide-Induced DNA Damage Response. *Toxicol Sci*.
- Galaz-Leiva S, Perez-Rodriguez G, Blazquez-Castro A, Stockert JC (2012) A simplified chromatin dispersion (nuclear halo) assay for detecting DNA breakage induced by ionizing radiation and chemical agents. *Biotech Histochem* 87: 208–217.
- Van Oorschot B, Oei AL, Nuijens AC, Rodermond H, Hoeben R, et al. (2013) Decay of gamma-H2AX foci correlates with potentially lethal damage repair and P53 status in human colorectal carcinoma cells. *Cell Mol Biol Lett*.
- Sun Y, Jin XL, Zhang TT, Jia CW, Chen J (2013) [MiR-150-5p inhibits the proliferation and promoted apoptosis of pancreatic cancer cells]. *Zhonghua Bing Li Xue Za Zhi* 42: 460–464.
- Kim KS, Kim JE, Choi KJ, Bae S, Kim DH (2013) Characterization of DNA Damage-Induced Cellular Senescence by Ionizing Radiation in Endothelial Cells. *Int J Radiat Biol*.
- John B, Enright AJ, Aravin A, Tuschl T, Sander C, et al. (2004) Human MicroRNA targets. *PLoS Biol* 2: e363.
- Garcia DM, Baek D, Shin C, Bell GW, Grimson A, et al. (2011) Weak seed-pairing stability and high target-site abundance decrease the proficiency of lsy-6 and other microRNAs. *Nat Struct Mol Biol* 18: 1139–1146.
- Rehmsmeier M, Steffen P, Hochsmann M, Giegerich R (2004) Fast and effective prediction of microRNA/target duplexes. *RNA* 10: 1507–1517.
- Smoot ME, Ono K, Ruscheinski J, Wang PL, Ideker T (2011) Cytoscape 2.8: new features for data integration and network visualization. *Bioinformatics* 27: 431–432.
- Kelder T, van Iersel MP, Hanspers K, Kutmon M, Conklin BR, et al. (2012) WikiPathways: building research communities on biological pathways. *Nucleic Acids Res* 40: D1301–1307.
- Keshava Prasad TS, Goel R, Kandasamy K, Keerthikumar S, Kumar S, et al. (2009) Human Protein Reference Database—2009 update. *Nucleic Acids Res* 37: D767–772.

Acknowledgments

Authors acknowledge SMVDU and J&K DST, India.

Author Contributions

Conceived and designed the experiments: SM KM PK NS RNKB. Performed the experiments: SM KM PK BK. Analyzed the data: SM KM PK. Contributed reagents/materials/analysis tools: RNKB. Contributed to the writing of the manuscript: SM KM PK RNKB.